

BROWNIAN COAGULATION OF AEROSOLS IN THE TRANSITION REGIME

M. KERKER, A. CHATTERJEE and D. D. COOKE
Clarkson College of Technology, Potsdam, NY 13676, USA

Abstract—Earlier experimental studies of Brownian coagulation of aerosols have been extended into the transition regime, i.e. Knudsen number values 0.8–1.6. This was done by working with the same range of particle size as earlier, but at a reduced pressure. A number of modifications were made in the experimental technique, including the use of diethylhexylsebacate instead of dibutylphthalate in order to avoid the possibility of loss to the walls by evaporation.

The rate of coagulation at $Kn = 0.2$ agreed closely with that predicted, using Smoluchowski's coagulation constant for the continuum regime as modified by the Cunningham correction. The rate at higher Knudsen numbers ($Kn = 0.8$ – 1.6) was somewhat lower (about 20%) than that predicted by Fuchs' formula for interpolation between the continuum and free molecule regimes.

Colloidal particles suspended in a fluid medium are constantly buffeted about due to the molecular impacts, and they trace out tortuous paths which we call Brownian motion. Whenever two such particles collide, they may either stick together or bounce apart. It is a one-way process—larger particles do not shatter into smaller ones—so that a fine-grained system inevitably becomes coarser. It coagulates.

The process is conceived as arising from two body collisions. Accordingly, the fundamental equation can be represented by

$$\frac{dn_k}{dt} = \frac{1}{2} \sum_{j=1}^{i=k-1} k(a_i, a_j) n_i n_j - n_k \sum_{i=1}^{\infty} k(a_i, a_k) n_i \quad (1)$$

when n_k is the concentration of particles with radius a_k . The first term represents the rate of formation of particles of size a_k by collision and subsequent coalescence of pairs of smaller particles, and the second term represents the rate of depletion of particles of this class by collision with all other classes.

The crux of the matter is the rate constant, $k(a_i, a_j)$. This depends upon a great many factors. However, we will simplify the problem considerably. Firstly, we assume that coagulation is only due to translational Brownian motion, eliminating all other processes that can bring particles into contact, such as the sliding of adjacent lamina past each other, turbulence, thermal gradients, molecular diffusional gradients, and electrical, magnetic and gravitational fields. We also assume that the particles are spherical, that they coalesce upon coming into contact, and that they are liquid so that the coagulum also assumes spherical shape.

Brownian motion of particles is conceived as originating from two aspects of the mechanical interaction with the fluid. At any particular moment there is a net impulse due to the non-uniformity of the molecular bombardment of the particle. At the same time, there is a resistance to the resultant motion of the particle which arises from the viscosity of the fluid.

There are three regimes. These depend upon a dimensionless parameter known as the Knudsen number, which is the ratio of the molecular mean free path in the fluid to the particle radius, $Kn = \lambda/a$. When $Kn < 0.1$, the so-called continuum treatment, in which a layer of fluid is dragged along with the particles, applies. In this case, the

particle motion is described by the Stokes–Einstein diffusion coefficient. For aerosols at atmospheric pressure, this corresponds to particle radii of approximately one micrometer or greater.

At sufficiently large values of the Knudsen number, there is no interaction between the particles and the fluid. Then the colloidal particles are conceived as undergoing a molecular-like motion obeying the kinetic molecular theory. A value of $Kn > 10$ is generally taken for the onset of this free molecular condition, corresponding either to very small particle sizes or very large molecular mean free paths.

Intermediate values of the Knudsen number ($0.1 < Kn < 10$) comprise the so-called transition regime for which there is no adequate theory. In this regime there is “slippage” between the particle and the fluid as a result of their relative motion. The slip effect can be corrected for in the first part of the transition regime ($0.1 < Kn < 0.5$) by an empirical correction to the diffusion coefficient, the Cunningham correction. This was studied by Robert Millikan, and the values proposed by him in 1923 are still in use today.

Smoluchowski set the problem up as a diffusion process. The rate of coagulation was related to the rate at which particles diffused toward a central particle. He utilized for the diffusion coefficient the value obtained by Einstein for a particle undergoing Brownian motion in the continuous regime, i.e. when $Kn < 0.1$. The resulting coagulation constant can be written as

$$k_s(a_i, a_j) = \frac{2kT}{3\eta} (a_i + a_j) \left[\frac{1}{a_i} + \frac{1}{a_j} \right] \quad (2)$$

where k is the Boltzmann constant, T is the Kelvin temperature, and η is the gas viscosity. Smoluchowski noted for the special case in which initially there is only one class of sizes, the coagulation equation reduces to a simple second order rate equation which is independent of particle size

$$-\frac{dn}{dt} = \frac{4kT}{3\eta} n^2 = 3.0 \times 10^{-10} n^2 \left(\text{at } \frac{T}{1 \text{ atm}} = 296^\circ\text{K} \right). \quad (3)$$

Indeed, until about a decade ago when computer based solutions of eqns (1) and (2) became practical, experimental studies of coagulation generally merely verified

whether or not the reciprocal of the particle number declined linearly with time in accordance with the well-known solution to the second-order rate equation.

For the initial part of the transition regime, the Cunningham correction enters in a straightforward manner, giving (for $0.1 < Kn < 0.5$)

$$k_C(a_i, a_j) = \frac{2kT}{3\eta} (a_i + a_j) \left[\frac{1}{a_i} \left(1 + A_i \frac{\lambda}{a_i} \right) + \frac{1}{a_j} \left(1 + A_j \frac{\lambda}{a_j} \right) \right] \quad (4)$$

The coagulation constant for the free molecule regime ($Kn > 10$) can be written as

$$k_M(a_i, a_j) = \left[\frac{8kT(m_i + m_j)}{m_i m_j} \right]^{1/2} (a_i + a_j)^2 \quad (5)$$

where m_i and m_j are the particle masses.

Perhaps the most useful interpolation between the continuous and free molecule theory has been worked out by Fuchs. The particles are assumed to diffuse in agreement with the continuum model to within a distance of the central particle comparable to the molecular mean free path. Within this spherical layer there is a "jump" in particle concentration in which diffusion occurs by the free molecule mechanism. The particle flux is matched at this surface of this layer. Although Fuchs' expression is rather complicated, it does not involve any new physical parameters, and so we will not write it out here, merely designating it as $k_F(a_i, a_j)$. The reader is referred elsewhere for the detailed expressions.¹

We now define a relative rate constant β by

$$\beta = k_S(a_i, a_j) \beta \quad (6)$$

β is the ratio of the coagulation constant for equal-size particles, as given by a particular theoretical expression, to the constant given by the Smoluchowski expression. Figure 1 is a plot of β against Kn as calculated by the

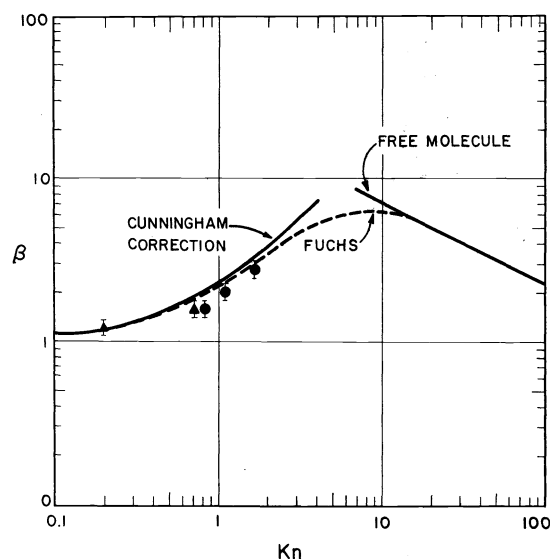


Fig. 1. Collision rates for equal size spheres relative to Smoluchowski's continuum result. Cunningham correction from eqn (4), Fuchs from reference [1], and free molecule from eqn (5). Triangles depict average values of β_E obtained with dibutylphthalate, circles depict average values of β_E obtained with diethylhexylsebacate.

various equations. The Cunningham expression takes effect as $Kn > 0.1$. The diagram illustrates how the Fuchs' expression interpolates between the two limits—the Smoluchowski and the free molecule cases—going through a maximum in the transition zone. The experimental points will be discussed later in this paper.

Experimental studies of coagulation have often been quite crude, being usually concerned with a qualitative verification of the second-order rate relation predicted by the initial rate of coagulation of a monodisperse system. There have been two categories of difficulties. The first is related to the preparation of narrowly dispersed colloids consisting of spheres which coalesce to spheres, and the second to the analysis of particle size distribution.

We have recently developed an aerosol generator which lends itself quite well to this problem and, in addition, have had considerable experience in aerosol particle size analysis by light scattering. We will not be able in this paper to consider the many aspects of aerosol generation involved in the design of the generator nor the equally interesting problems related to particle size analysis by light scattering. We utilized a procedure in which light scattering "monitors" the evolution of the particle size distribution. It was not possible to determine the size distribution *ab initio* because of the complexity of the size distribution of a coagulated system.

Our strategy was as follows. The light scattering was measured early enough in the life history of the aerosol for its size distribution to be monomodal and sufficiently narrow to obtain an unambiguous determination of the particle size distribution. The scattered light was also measured at some later time during which coagulation had occurred. The latter light-scattering results were not utilized directly; rather, starting with the initial distribution, the evolution of the particle size distribution with time was calculated using the Fuchs' kernel in the coagulation equation. The particle size distribution at each particular time had a characteristic light-scattering pattern associated with it. The coagulation time was advanced until the light-scattering pattern calculated in this way agreed with the pattern which had been measured at the later time.

Another experimental strategy on which we had to decide was the manner of varying the Knudsen number. This, of course, is the variable that we wish to study. An obvious procedure is to work with aerosols of different particle sizes. This is easier said than done. There is a lower size limit of about $0.15\text{--}0.20\ \mu\text{m}$ which is imposed by the light-scattering technique. This would limit us to an upper value of the Knudsen number which would be less than unity. However, there is another way of scaling the Knudsen number, *viz* to alter the mean free path of the gas. The latter procedure has the advantage that a particle size range can be selected which is convenient both from the point of view of aerosol generation and of particle size analysis. The mean free path was altered by working at reduced pressures. This required changes in the design of our aerosol generator as well as in several of the measuring techniques.

The experimental assembly is shown schematically albeit not to scale, in Fig. 2. It is a flow system in which there are no constrictions or sharp bends so that laminar flow is obtained throughout. It may be operated from atmospheric pressure to moderately reduced pressures; in the experiments being reported here, the pressure ranged from 0.5 to 1 atm. All light-scattering measurements were made *in situ* without perturbing the system.

The apparatus consists of the following sections: (1) an

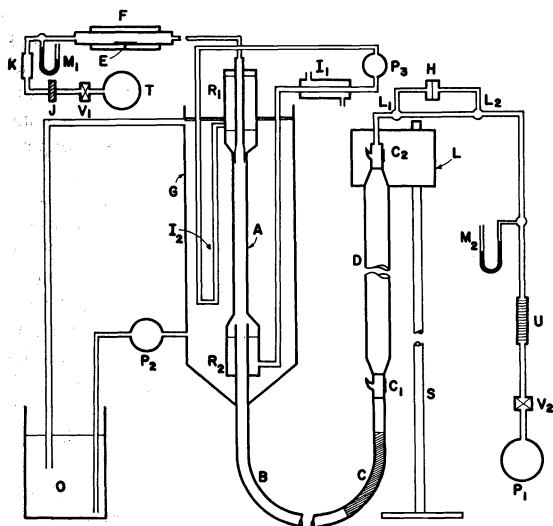


Fig. 2. Schematic diagram (not to scale) of apparatus. Helium tank, T, needle valves, V_1 , V_2 , glass-wool filters J, U, flowmeter K, mercury manometers M_1 , M_2 , combustion furnace F, combustion boat E, falling film evaporator A, reservoirs for DEHS R_1 , R_2 , heat exchanger I_1 , tube for reheating DEHS I_2 , tube pump P_3 , oil bath G, oil thermostat O, rotary pump P_2 , condensation zone B, reheating and condensation zone C, light scattering cells C_1 , C_2 , hold-up tube D, light scattering photometer L, by-pass valves L_1 , L_2 , millipore filter holder H, vacuum pump P_1 .

aerosol generator, (2) a coagulation chamber, (3) a light scattering photometer, (4) a filter sampler, and (5) a pumping system.

Helium is the carrier gas. It passes through furnace F maintained at 590°C where it picks up AgCl vapor from molten AgCl contained in combustion boat E. This vapor condenses to minute aerosol particles which serve as condensation nuclei.

The heart of the generator is tube A, down the walls of which drains a film of diethylhexylsebacate (DEHS). It is important for the proper functioning of this generator that this film flows uniformly and continuously along the walls of this container. The DEHS is recycled from reservoir R_1 to reservoir R_2 by means of a tube pump P. This section of the generator is maintained at an elevated temperature (e.g. 167°C) by circulating hot silicone oil from the oil bath A through the thermostat O by means of a rotary pump P_2 . It is necessary to operate this generator at such a high temperature because of the exceedingly low vapor pressure of DEHS, which at room temperature is about 10^{-9} mm. This is sufficiently low so that there is no possibility of evaporation of the aerosol with subsequent condensation upon the walls of the coagulation chamber. Accordingly, all changes in particle size may be ascribed to coagulation.

The nuclei-laden helium stream becomes partially saturated with DEHS vapor in tube A, and the vapor condenses upon the AgCl nuclei as it emerges from the heated zone in tube B. This initial aerosol is then reevaporated in tube C, which is heated to 265°C by electrical heating tape, and the final quite monodispersed aerosol reforms upon emerging into the cool zone.

Two light scattering cells, C_1 and C_2 , each equipped with a flat entrance window and a Rayleigh horn, are attached by ground glass joints at the entrance and at the exit of the hold-up tube D. Figure 3 illustrates these cells schematically. These cells have the same diameter as tube

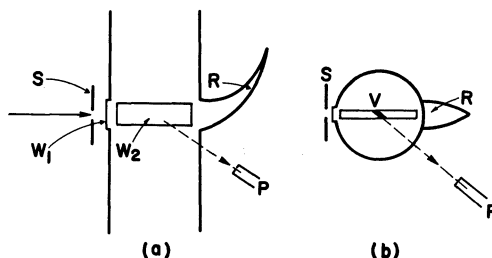


Fig. 3. Illuminated region view by photometer P; entrance slit S, entrance window W_1 , viewing window W_2 , Rayleigh horn R, region view by photometer, V. (a) side view; (b) top view.

B, and with the gradual tapers at the entrance and the exit of the hold-up tube, there is no apparent turbulence in the aerosol stream. The aerosol exhibits brilliant higher order Tyndall spectra under white light illumination.

Light-scattering measurements were obtained with the aid of a specially constructed photometer which is capable of sliding along the stand S. This apparatus was designed to clear the hold-up tube and the light-scattering cells so that *in situ* measurements could be made at each location. At the entrance to the hold-up tube, prior to significant amount of coagulation, the aerosol is relatively monodisperse. There were several hold-up tubes each with a different volume. The coagulation times depended upon the particular hold-up tube and the flow rate.

The entire assembly between the needle valves V_1 and V_2 was kept under the desired reduced pressure by careful adjustment of the helium flow rate at V_1 and V_2 , and also of the pumping rate of P_1 .

The aerosol mass concentration was measured gravimetrically. We noted that there was a radial concentration gradient in the tube, and that this varied with pressure. The gradient occurs because cooling starts in the outer regions of the tube, and as condensation starts there is diffusion of vapor from the axial region until this region cools sufficiently for condensation to occur. Since the light-scattering measurements occur in the axial region, it was necessary to measure the concentration specifically in that region, and this was done with the sampling device illustrated in Fig. 4. The experimental details of these measurements, as well as a number of other experimental problems that had to be surmounted, are described elsewhere.¹

The calculation is outlined in Fig. 5. Light-scattering data obtained prior to entry into and after exit from the hold-up tube are depicted in the upper two boxes. The first step is the inversion of the data at the entry in order to obtain the size distribution of the initial aerosol. This is characterized by two parameters, the modal radius and a measure of the width of the distribution. In addition, the particle concentration is calculated from the mass concentration obtained from filtration data and from the study of the variation of concentration in the central region compared with the total concentration.

The second step is the calculation of the size distribution as a function of coagulation time. This was done in two ways—using the Smoluchowski collision kernel with Cunningham correction, and also with the Fuchs' interpolation formula.

In this calculation it is necessary to remember that aerosol is undergoing Poiseuille flow with the usual parabolic velocity profile. Generally, the coagulation equations must be solved separately for each annular region, and the size distribution which is obtained for each

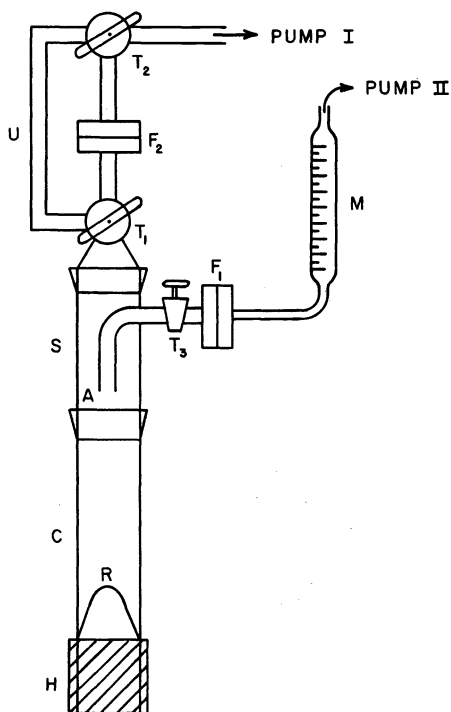


Fig. 4. Sampler for determination of aerosol concentration in axial region; sampler S, condenser C, heating tape H, flowmeter M, filters F_1 and F_2 , axial sampling tube A, aerosol reformation zone R, stopcocks T_1 , T_2 and T_3 , bypass U.

annulus must be averaged appropriately to obtain the final distribution. Actually, since we are only interested in the aerosol within the illuminated region viewed by the photometer, the calculation need only consider a sufficient number of annuli to encompass this region. In fact, it is only the fraction of each annulus cut by the view of the phototube that is actually averaged. This varies with the angle of observation.

The polarization of the scattered light corresponding to the size distribution within the viewing volume of the

photometer is then calculated for each angle of observation. This comprises step 3. Step 4 consists in comparing the calculated polarization ratio with the experimental light-scattering data depicted in the upper right box in Fig. 4. The coagulation time is then advanced until the two sets of light-scattering data (the calculated and the experimental) best agree. The criterion of a best fit is a minimum in the mean square per cent deviation of the 19 experimental and calculated values of the polarization. Obviously, this is an arduous calculation.

We have completed experiments and calculations for a large number of runs at three pressures, viz. 1 atm, $\frac{1}{2}$ atm, and $\frac{1}{4}$ atm. Four different hold-up tubes and three different flow rates were utilized in order to vary the results. These actually involved rather short coagulation times in order to avoid working with highly polydisperse systems. In most cases, this meant less than a quarter-life time, and although the size distributions broadened significantly, there was not a very great change in the average size.

Tables 1-3 illustrate the results obtained with DEHS at each of the pressures which have been investigated. The average residence time in each hold-up tube is given by t_E ; t_F represents the calculated average residence time, using Fuchs' equation, which leads to agreement between the calculated and the measured polarization of the scattered light. The corresponding quantity using the Smoluchowski-Cunningham equation is given by t_C . Fuchs' equation predicts slightly more rapid coagulation than is observed; the Smoluchowski-Cunningham equation predicts a greater deviation.

The Fuchs' collision rate, β_F , is defined above in terms of the modal size in the distribution. It is the rate predicted by the Fuchs equation relative to that predicted by the Smoluchowski equation for the rate constant. The experimental rate, β_E , given in the last column of each table is defined by

$$\beta_E = \beta_F(t_F/t_E). \quad (7)$$

Accordingly the use of t_F/t_E as an empirical correction factor will give coagulation times in agreement with experiment.

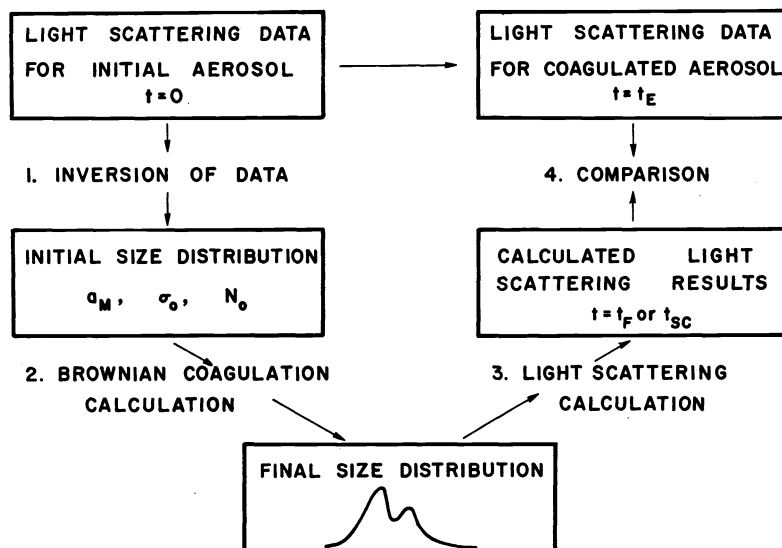


Fig. 5. Flow chart for coagulation calculation. Calculation is complete when light scattering data for coagulated aerosol agrees with calculated light scattering results. Experimental hold-up time is t_E . Calculated hold-up times obtained using the Fuchs equation is t_F ; that obtained with Smoluchowski-Cunningham equation is t_C .

Table 1. Theoretical and experimental coagulation results (pressure 761 ± 5 mm; temp $24.6 \pm 0.5^\circ$; flow rate 1.0 l/min)

Modal radius (μ m)	Breadth parameter (σ_0)	Knudsen number (Kn)	Experimental time (t_E)	Fuchs' time (t_F)	Smoluch.-Cunningham time (t_C)	Fuchs' collision rate (β_F)	Experimental collision rate (β_E)
0.23	0.07	0.84	47	35	34	2.05	1.54
0.24	0.07	0.80	47	41	39	1.99	1.77
0.23	0.09	0.84	47	39	36	2.05	1.72
0.23	0.07	0.81	47	41	39	2.02	1.78
0.23	0.10	0.84	47	38	36	2.06	1.68
0.23	0.10	0.84	81	57	51	2.05	1.44
0.23	0.07	0.85	81	64	61	2.07	1.64
0.23	0.07	0.85	81	65	61	2.07	1.66
0.23	0.07	0.83	81	50	47	2.03	1.25
0.24	0.08	0.81	107	82	77	2.02	1.55
0.23	0.08	0.83	107	84	78	2.04	1.60
0.24	0.08	0.81	107	82	78	2.02	1.55
0.23	0.07	0.84	107	82	77	2.05	1.57
0.24	0.07	0.82	107	73	68	2.02	1.38
0.23	0.13	0.84	152	123	118	2.04	1.66
Average	0.23	0.08				2.04	1.59
S.D.	0.01	0.01				0.02	0.14

Table 2. Theoretical and experimental coagulation results (pressure 569 ± 4 mm; temp $24.1 \pm 1.4^\circ$; flow rate 1.35 l/min)

Modal radius (μ m)	Breadth parameter (σ_0)	Knudsen number (Kn)	Experimental time (t_E)	Fuchs' time (t_F)	Smoluch.-Cunningham time (t_C)	Fuchs' collision rate (β_F)	Experimental collision rate (β_E)
0.23	0.09	1.11	68	56	53	2.42	1.99
0.24	0.10	1.07	68	68	61	2.38	2.38
0.23	0.10	1.12	68	59	57	2.44	2.12
0.23	0.11	1.12	68	51	50	2.44	1.83
0.23	0.10	1.11	61	43	43	2.42	1.71
0.23	0.11	1.15	61	43	38	2.48	1.75
0.23	0.09	1.11	61	52	49	2.43	2.07
0.23	0.08	1.11	61	60	57	2.43	2.39
0.24	0.10	1.08	61	58	55	2.39	2.27
Average	0.23	0.10				2.43	2.06
S.D.	0.01	0.01				0.03	0.24

Table 3. Theoretical and experimental coagulation results (pressure 385 ± 6 mm; temp $25.1 \pm 0.8^\circ$ C; flow rate 2.03 l/min)

Modal radius (μ m)	Breadth parameter (σ_0)	Knudsen number (Kn)	Experimental time (t_E)	Fuchs' time (t_F)	Smoluch.-Cunningham time (t_C)	Fuchs' collision rate (β_F)	Experimental collision rate (β_E)
0.23	0.12	1.67	45	39	36	3.20	2.77
0.24	0.13	1.63	45	37	37	3.16	2.60
0.23	0.12	1.70	41	39	35	3.25	3.09
0.24	0.12	1.58	41	35	35	3.08	2.63
0.23	0.14	1.65	85	69	65	3.17	2.57
0.23	0.14	1.67	85	61	58	3.20	2.30
0.23	0.15	1.72	85	81	65	3.26	3.11
0.23	0.13	1.68	85	83	76	3.21	3.13
Average	0.23	0.13				3.19	2.78
S.D.	0.01	0.01				0.04	0.29

The points on Fig. 1 summarize the averages of the results of five sets of experiments, including two earlier sets with dibutylphthalate aerosols, one set in nitrogen as the carrier gas and one in helium. The points in this figure correspond to β_E in the tables.

Fuchs' equation may be viewed as a semi-theoretical interpolation formula; in a sense, the purpose of this research has been to check its validity. For $Kn = 0.20$,

where the Cunningham correction is not very large (about 25% correction to the diffusion coefficient), the experimental rate agrees very closely with the theoretical value obtained by using the Cunningham correction in Smoluchowski's equation. Little can be said in this case about the coalescence efficiency. This is because the coagulation rate is not sensitive to coalescence efficiency whenever the radius of the aerosol particle is large

compared to the stopping distance for the particle, as is the case here.

At the next higher value of Knudsen number ($Kn = 0.83$), the agreement between the two sets of results is remarkably good despite changes in the experimental procedure which included (1) changing the aerosol material from DBP to DEHS with concomitant changes in the aerosol generator and changing the procedure for analyzing the mass concentration, (2) changes in the optics, and (3) changes in the computations.

The averaged results at each of the higher Knudsen numbers ($Kn = 0.78, 0.83, 1.10$ and 1.66) indicate that Fuchs' equation over-corrects the rate constant in this

range by about 20%. This might suggest that the coalescence efficiency is less than unity. However, considering the approximate nature of the equation and the experimental error of about 10%, we would stress the agreement between Fuchs' equation and experiment rather than the difference. Work is continuing at lower pressures, i.e. at higher Knudsen numbers.

Acknowledgement—This work has been supported by NSF Grant GP33654X.

REFERENCES

¹A. Chatterjee, M. Kerker and D. D. Cooke, *J. Colloid Interface Sci.* **53**, 71–82 (1975).